Photofragment Spectrum of C-State HCN. Theoretical Interpretation

David T. Chuljian† and Jack Simons*

Contribution from the Department of Chemistry, University of Utah, Salt Lake City, Utah 84112. *Received May 27, 1981*

Abstract: We have made use of an ab initio configuration interaction energy surface for the C state of HCN to interpret the experimental fluorescence spectrum of B state ($^2\Sigma^+$) CN produced by the photodissociation of HCN and DCN. Most of the experimental data, which previously had not been interpreted, can be explained by using our surface in conjunction with a simple tunneling model of the dissociation process. For low-level excitation of the bending vibration (v_2), i.e., small angular deviation from equilibrium, the surface's shape in the radial R(H--CN) direction is such that the C state is either bound or purely dissociative. For higher values of v_2, the molecule populates regions of the energy surface which have barriers in the dissociation direction. Our model predicts variation of the photodissociation behavior as a function of excitation of the H--CN stretching vibration (v_1) and agrees well with experiment, except for the v_2 progression of DCN with $v_1 = 2$. Possible reasons for this single disagreement are discussed.

Recent experimental data on the photofragmentation of C-state HCN to produce excited $^2\Pi$ and $^2\Sigma^+$ CN radicals[1] has not been fully interpreted in terms of the relevant HCN potential energy surfaces. It was this unexplained experimental data which motivated us to undertake the series of ab initio calculations reported in this paper. In the Simons and MacPherson photofragmentation experiment,[1] it was noted that, within the absorption band of HCN starting near 145 nm (which gives the C state), the rates of predissociation of HCN and DCN were sufficiently slow as to permit experimental resolution of a long progression in the bending mode (v_2) as long as the H--CN stretching mode (v_1) was not excited. For $v_1 > 0$, HCN dissociated much more rapidly than DCN and so quickly than no v_2 progression could be observed. DCN, however, supports v_2 progressions for $v_1 \leq 2$. These facts were used to infer that the C state has a barrier along the R(H--CN) coordinate with a height less than 4000 cm^{-1} which approximately corresponds to the $v_1 = 1$ energy of HCN (3400 cm^{-1}).[2] However, the $v_1 = 2$ energy of DCN (3600 cm^{-1}) is even *greater* than the $v_1 = 1$ energy of HCN. This leads one to ask why $v_1 = 2$ DCN should show predissociative behavior (indicative of a lifetime of about 10^{-13} s) whereas $v_1 = 1$ HCN is entirely dissociative (i.e., has a much shorter existence). Certainly it is possible, although not probable, that the barrier on the C-state surface is of *precisely* the correct height and thickness to permit rapid HCN tunneling but only slow DCN tunneling.

There are other interesting features in Simons and MacPherson's photofragmentation data. The lack of a strong isotope effect for $v_1 = 0$ was considered puzzling because it was expected that if simple tunneling were dominant, then the bending mode (v_2) progression with $v_1 = 0$ should show the *largest* isotope effect, since for $v_1 = 0$ the radial barrier would be "thickest". However, the experimental data show little isotope effect for $v_1 = 0$. Simons and MacPherson therefore proposed that another parallel and independent dissociation pathway must exist. They suggested that for $v_1 > 0$ for HCN ($v_1 > 2$ for DCN) the R(H--CN) tunneling dominates, whereas for $v_1 = 0$ ($v_1 \leq 2$ for DCN) the R(H--CN) tunneling is slow and the alternative competing path dominates.

By measuring the degree to which the initial polarization of the C state, which is induced by the polarization of the absorbed photon, is retained in the CN B $^2\Sigma^+$ fragment, Simons and MacPherson estimated the *lifetimes* of the $v_1 = 0$ and $v_1 > 0$ C-state HCN molecules to be 2.0×10^{-13} and 2.0×10^{-14} s, respectively. The shorter lived HCN molecules were thought to have been formed in a faster process which was attributed to the R(H--CN) tunneling. The (slower) competing process, which presumably was operative for $v_1 = 0$ for HCN ($v_1 \leq 2$ for DCN), seemed to be accelerated when the bending mode was excited. Simons and MacPherson left open, however, the physical nature of the competing mechanism. It was with this background of experimental facts and mechanistic proposals that we began our investigations. As will be shown, we think our potential energy surface has let us characterize the nature of the "competing pathway".

Overview of Calculations on HCN C State

Several other workers have performed ab initio calculations on the low-lying excited electronic states of HCN.[3-9] Pertinent results of Vazquez and Gouyet,[6,7] Schaefer et al.,[8] and Peyerimhoff et al.[9] are discussed later. In this paper, we limit our consideration to the singlet excited states of HCN because they presumably are the experimentally relevant states. We further restrict our treatment to those states which are of A′ symmetry in the C_s point group because measurements of the CN polarization ratios led Simons and MacPherson[1] to assign A′ symmetry to the C state. We have considered a wide range of molecular geometries in which R(H--CN) and θ(HCN) are varied with R(HC--N) being held fixed near the equilibrium bond length of the B $^2\Sigma^+$ CN radical produced in the photofragmentation of C-state HCN. This restriction to fixed HC--N bond length limits us to exploring that part of Simons and MacPherson's photofragment spectrum in which the HC--N stretching mode (v_3) is not excited. This is not a serious limitation because it still permits us to explore the nature of the proposed competitive dissociation channel (which, as the experimental data indicate, exists even when $v_3 = 0$).

Although the basis set and the size of the configuration interaction (CI) wave function employed here are not state of the art, we have attempted to treat all portions of the C-state potential-energy surface with equal precision (see later for a description of how this was achieved).

Our intent is not to generate a highly accurate ab initio surface with which to *predict* observable phenomena. Rather, we want to obtain a qualitatively correct global picture of the electronic surface, so that we can interpret the available experimental data. If our surface gives bound, predissociating, and unbound energy

† University of Utah Graduate Research Fellow.
* J. S. Guggenheim Fellow, D. P. Gardner Fellow.

(1) M. T. MacPherson and J. P. Simons, *J. Chem. Soc., Faraday Trans. 2*, **74**, 1965 (1978).
(2) G. Herzberg, "Electronic Spectra of Polyatomic Molecules", Van Nostrand, New York, 1966, p 588.
(3) G. M. Schwenzer, C. F. Bender, and H. F. Schaefer III, *Chem. Phys. Lett.*, **36**, 179 (1975).
(4) A. Rauk and J. M. Barriel, *Chem. Phys.*, **25**, 409 (1977).
(5) G. J. Vazquez and J. F. Gouyet, *Chem. Phys. Lett.*, **57**, 385 (1978).
(6) G. J. Vazquez and J. F. Gouyet, *Chem. Phys. Lett.*, **65**, 515 (1979).
(7) G. J. Vazquez and J. F. Gouyet, *Chem. Phys. Lett.*, **77**, 233 (1981).
(8) G. M. Schwenzer, S. V. O'Neill, H. F. Schaefer III, C. P. Baskin, and C. F. Bender, *J. Chem. Phys.*, **60**, 2787 (1974).
(9) M. Peric, S. D. Peyerimhoff, and R. J. Buenker, *Can. J. Chem.*, **55**, 3664 (1977).

0002-7863/82/1504-0646$01.25/0

levels which follow the trends observed in the photofragment spectrum,[1] which contains on the order of 100 lines, we conclude that our surface is capable of giving insight into the nature of the photodissociation process for this particular system.

To help us visualize the energy surface, we performed fits of the C-state surface using a generalization of the multidimensional interpolation method of Downing et al.,[10] which permits one to simultaneously utilize information on two or more electronic states which are strongly interacting (details of the interpolation method are given in Appendix 1). We now describe in more detail the strategy and methods used in performing the ab initio calculations and in arriving at our final description of the C-state potential-energy surface.

A. Orbital and Configuration Considerations. The ground state of HCN is linear and of $^1\Sigma^+$ symmetry, but the excited C state is bent and of $^1A'$ symmetry in the C_s point group. We therefore display in Figures 1a and 2a the qualitative orbital correlation diagrams (OCD) of HCN at linear and bent geometries. The corresponding singlet configuration correlation diagrams (CCD) are shown in Figures 1b and 2b. The three lowest states of A′ symmetry we label the X, B, and C states, the C state being of $^1\Sigma^+$ symmetry in linear geometry. In constructing these CCD's, which are not meant to be highly accurate, we made use of the CN state energies (X $^2\Sigma^+$, A $^2\Pi$, and B $^2\Sigma^+$) given by Herzberg[11] as well as the results of calculations by Vazquez and Gouyet[6] and Peyerimhoff et al.[9] Clearly, in the linear geometry there are numerous crossings between configurations of the same and different symmetry, which we expect to give rise to symmetry-imposed barriers in the C-state dissociation process.

For the bent HCN molecule, the orbitals have a′ or a″ symmetry and hence only A′ and A″ states can result. Note the CCD appropriate to an angle of 125°, shown in Figure 2b (only configurations of $^1A'$ symmetry have been included): compared to the linear case, the H-atom orbital of the fragments now correlates with a lower energy orbital in HCN (an a′ π^*_{CN} orbital). As a result, the symmetry barrier to dissociation of bent C-state HCN is expected to be somewhat lower than in the linear case.

Because at linear geometries the B and C states arise from states of different symmetries ($^1\Delta$ and $^1\Pi$, respectively), whereas they both are of $^1A'$ symmetry in the (bent) C_s point group, a "conical intersection" is expected. That is, the B and C states may cross (as functions of R(H--CN)) because they are of different symmetries in the C_v point group, but they must undergo an avoided crossing once the molecule bends. The resulting symmetry imposed barrier in the lower B state is expected to be important in determining its dissociation behavior. At geometries near the barrier in the B state, a *minimum* is expected to occur in the higher energy C state. A barrier in the C state surface itself is also expected because of *other* avoided crossings (for example, with the D state). The expected behavior of the X, B, and C states is summarized in Figures 1c and 2c where the state correlation diagrams (SCD) are shown for linear and near-linear (θ = 175°) geometries and for the strongly bent (θ = 115°) geometry.

Because we are interested in obtaining a qualitatively correct global picture of the C-state potential surface (as θ and R(H--CN) vary), we must include in our configuration interaction (CI) calculations *all* configurations which contribute significantly to this state at any geometry. Near its equilibrium geomery, the C state is dominated by n → π^* character. However, the avoided crossings it undergoes involve states dominated by $\pi \rightarrow \pi^*$ character. Hence, we must be sure to allow for both kinds of charge distributions when carrying out our CI study.

B. Details of the ab Initio Calculations. 1. Basis Sets. The atomic orbital basis sets chosen for this work consisted of Dunning's (4s,2p) contractions of the (9s,5p) primitive Gaussian basis sets for carbon and nitrogen and Dunning's (3s) contraction of the (4s) Gaussian basis set for hydrogen.[12] This is essentially

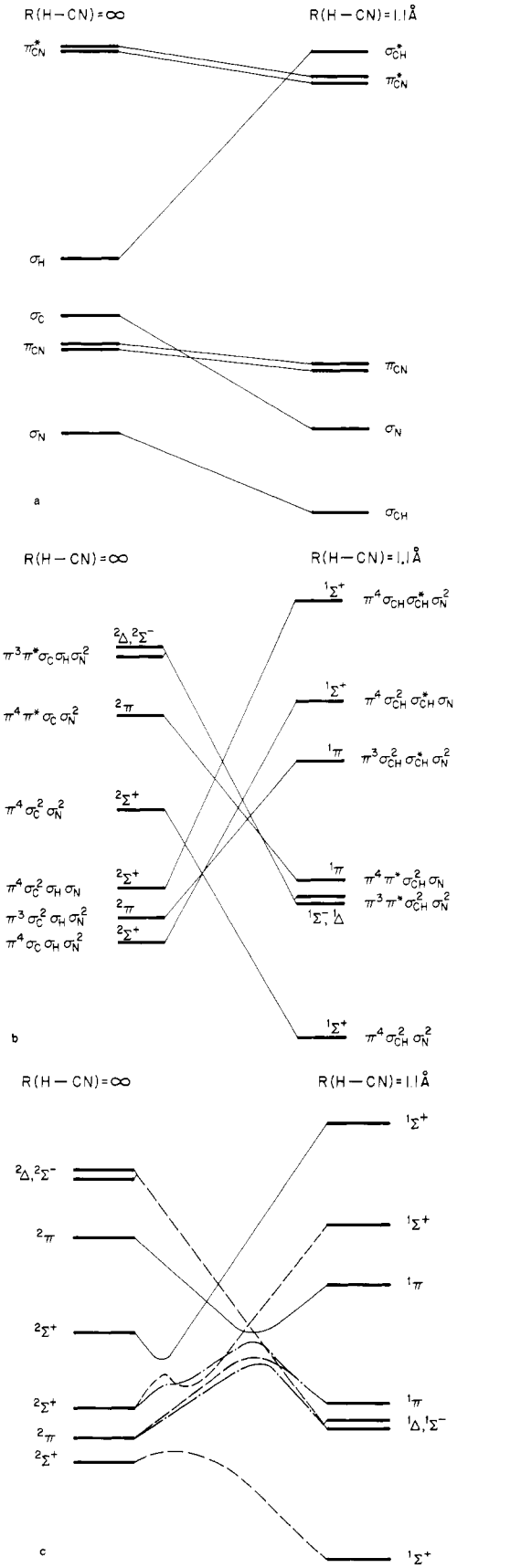

Figure 1. (a) Orbital correlation diagram (OCD) for the linear case. R(HC---N) is fixed at 2.2 bohr. (b) Configuration correlation diagram (CCD) for the linear case. State labels on left-hand side refer to the CN moiety; the H atom is always ^2S for configurations of interest. (c) State correlation diagram (SCD) for the linear (--) and near linear (-·-) cases (θ = 180° and 175°, respectively). For the near linear case, only states of A′ symmetry are shown for simplicity. States indicated by solid lines are not important for later calculations.

(10) J. W. Downing, J. Cizek, J. Paldus, and J. Michl, *Chem. Phys. Lett.*, **67**, 377 (1979).

(11) G. Herzberg, "Spectra of Diatomic Molecules", Van Nostrand, New York, 1950, p 520.

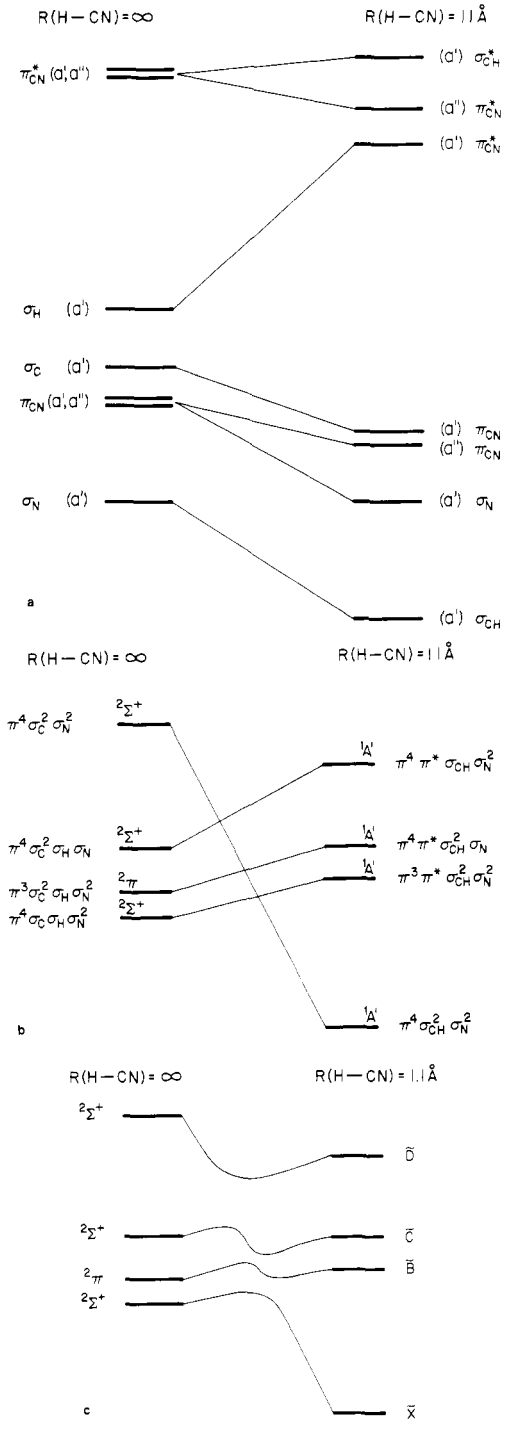

Figure 2. (a) OCD for the strongly bent (θ = 125°) case. (b) CCD for the strongly bent case. Only configurations of A′ symmetry for HCN (and their correlating configurations in the fragments) are shown. (c) SCD for strongly bent case. Only A′ states shown.

the same basis used by Schaefer et al.[8] in their study of HCN. For comparison, Peyerimhoff et al.[9] used a similar basis but with a p function on hydrogen in place of one of our s functions, and with one bond function of s symmetry in each of the CN and CH bonds. The SCF energy of Peyerimhoff et al. for the X $^1\Sigma^+$ state was −92.8467 au, whereas we obtained −92.8381 in our basis (Schaefer et al. did not publish their SCF energies). Vazquez and Gouyet[7] used a basis of 20 Slater functions of 4-31G quality; their SCF energy for the ground state was −92.7311 au. We think that our basis is comparable in quality to those used previously on HCN. Certainly it is *not* good enough to guarantee high quality

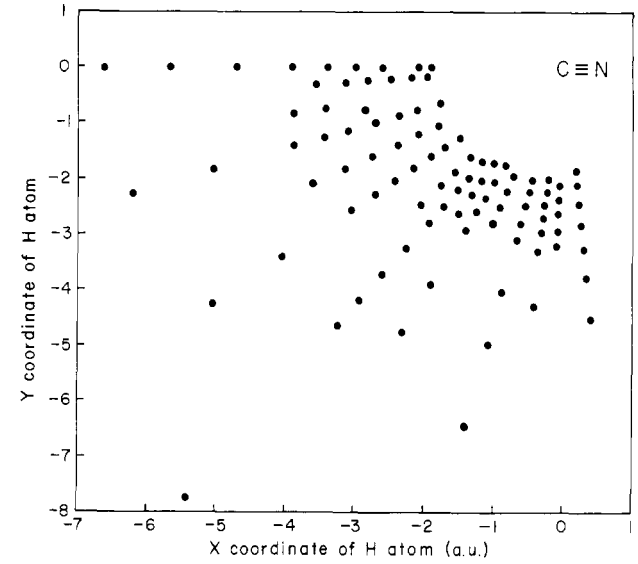

Figure 3. Geometries at which CI energies were calculated. Molecule is placed in *xy* plane with C atom at the origin and N atom on the positive *x* axis.

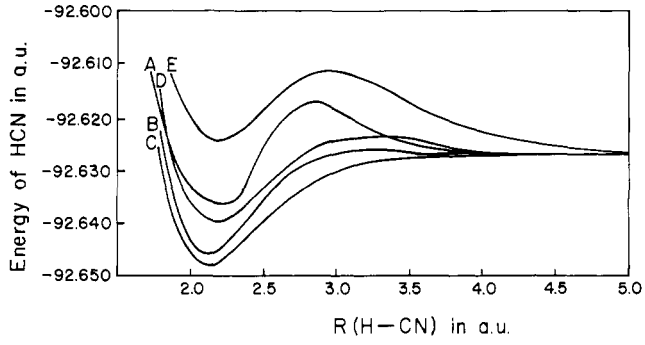

Figure 4. C-state dissociation sections for several angles. A, θ = 170°; B, θ = 155°; C, θ = 140° (equilibrium angle); D, θ = 110°; E, θ = 95°. Energy scale offset by +92 au.

(0.2 eV) absolute energies. However, that kind of accuracy is, as we show later, not necessary to rationalize Simons and MacPherson's puzzling experimental data.

2. CI Level Studies. Our CI calculations were performed using the unitary group based "direct CI" program written by Shepard.[13] In this approach, configuration lists are constructed by specifying occupation restrictions rather than by listing the specific Slater determinants to be used.

The procedure most often used to select configurations for inclusion in the CI calculation is not easily employed in the unitary group method. We therefore decided to select configurations on the basis of their coefficients in the CI wave function expansions at certain crucial "test" geometries. This method, which is detailed in Appendix 2, resulted in a 2488 configuration CI wave function which we used to generate all of the C-state energies reported in this work.

The 2488 configuration CI calculations were carried out at the geometries depicted in Figure 3. At several points on this geometry grid, the CI eigenvectors were examined to be sure that the configurations presumed to be dominant remained dominant. For angles less than 90°, the configuration list began to be somewhat less satisfactory in the sense that configurations with significant expansion coefficients (0.08–0.10) in the C-state CI eigenvector did not have all of their corresponding single and double excitations present in the configuration list. Therefore, although we carried out additional calculations for θ smaller than 90°, the energy surface should be considered less accurate in this region.

(12) T. H. Dunning, Jr., *J. Chem. Phys.*, **53**, 2823 (1970).

(13) R. Shepard, *Int. J. Quantum Chem., Symp.*, **14**, 211 (1980).

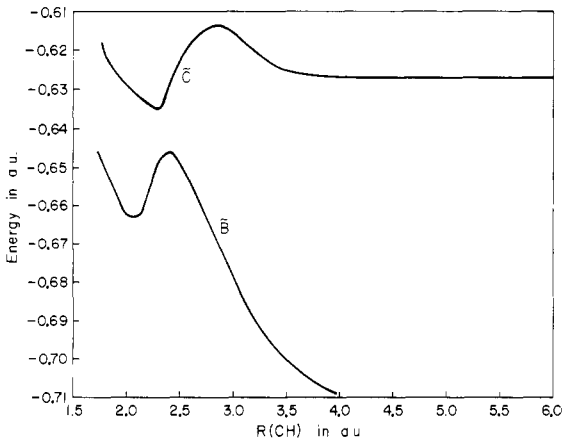

Figure 5. Dissociation sections for B and C states at $\theta = 180°$ (linear). Energy scale offset by +92 au.

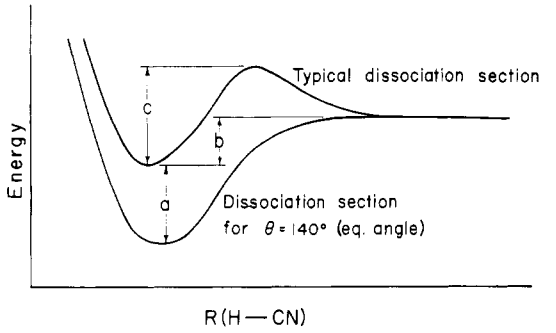

Figure 6. Dissociation sections defining values listed in Table I. Quantities *a*, *b*, and *c* correspond to the numbers in columns two, three, and four of Table I.

Results and Interpretation of Experimental Data

Several interpolated potential curves for the C state (at a variety of angles) are shown in Figure 4. Notice that near the C state equilibrium angle (140°) tunneling *cannot* occur; there is no barrier through which it can take place. Only for angles significantly far from 140° ($\theta > 160°$, $\theta < 120°$) do the potential-energy curves show barriers that could lead to tunneling.

Space limitations preclude showing dissociation sections for all angles where ab initio calculations and interpolations have been performed. The most important facts about each such curve are the barrier height (if there is a barrier) and the energy of the well's minimum (E_{min}) relative to the dissociation limit (E_∞) and relative to the energy of the C-state equilibrium geometry ($\theta = 140°$). This information has been abstracted from a "complete" set of our calculated curves and is shown in Table I. If we tentatively assume complete decoupling of the bending (v_2) and stretching (v_1) modes (which is reasonably justified by most of the Simons and MacPherson data), we can divide into three cases the situations which arise for any given value of the stretching quantum number v_1. First, *tunneling* can occur when the stretching mode contains enough energy to lie below the top of the barrier but above the asymptotic limit (R(H--CN) $\rightarrow \infty$). In this case, we expect predissociation (i.e., photofragmentation should occur but with spectral lines whose width is determined by the tunneling rate). Second, if v_1 is large enough that the energy in the stretching mode exceeds the barrier's top (or, if there is no barrier, the dissociation energy at that angle), very diffuse spectral features caused by *purely dissociative* transitions are expected. Third, at angles where no barrier exists, we expect to see structure in the *absorption* spectrum, but no appearance of H + CN product fluorescence if the energy in the v_1 mode is less than the dissociation energy at that angle. Based on this classification of the R(H--CN) motion, we now attempt to interpret the experimental data using our C state surface.

Table I indicates that tunneling should not occur at all until θ deviates appreciably from 140°. In Table II we give the angles at which the bending vibrations are expected to undergo their classical turning points for various values of v_2 for HCN and DCN. By combining this information with that of Table I, we can predict for which v_1,v_2 combinations predissociation should occur. Experimentally,[1] for $v_1 = 0$, HCN predissociation (as seen by $^2\Sigma^+$ CN fluorescence) began only when v_2 exceeded 4. The $v_2 = 5$

Table I. Summary of Information from Complete Set of Dissociation Sections[a]

θ, deg	$E_{min}(\theta) - E_{min}$(eq), cm^{-1}	$E_\infty - E_{min}(\theta)$, cm^{-1}	barrier height, cm^{-1}
180	2500	2000	4980
175	2500	2000	4980
170	2440	2060	4190
165	1780	2720	3990
160	990	3510	4080
155	460	4040	4210
150	90	4410	4410
145	0	4500	4500
140	0	4500	4500
135	150	4350	4350
130	400	4100	4100
125	660	3840	3840
120	990	3510	3620
115	1300	3200	3600
110	1760	2740	3560
105	2460	2040	3470
100	3530	970	3230
95	5070	−570	2880
90	7050	−2550	2500
85	9810	−5310	1980
80	13850	−9350	790

[a] $E_{min}(\theta)$ indicates lowest value of energy of molecule restricted to a given angle θ, E_{min}(eq) indicates the minimum energy on the dissociation section at the optimum angle (140°); E_∞ is the energy of HCN dissociated to B state CN and ^{2}S hydrogen. Figure 6 illustrates these parameters for a typical dissociation section.

Table II. Turning Points for H (D) Atom Moving along Calculated $E_{min}(\theta)$ Path (See Figure 6) with CN Fragment Fixed as Shown in Figure 3

	classical angular turning points for bending vibration,[a] deg				
	HCN		DCN		
$v_2 = 0$	129.0	154.0	131.0	153.0	
1	116.0	161.0	120.0	160.0	
2	108.2	166.0	113.0	164.0	
3	103.0	180.0[b]	106.4	169.0	
4	99.6	180.0	102.8	180.0	103.1[c]
5	97.0	180.0	99.6	180.0	
6	94.4	180.0	97.6	180.0	
7	92.6	180.0	95.6	180.0	95.7
8	90.7	180.0	93.9	180.0	94.0
9	89.2	180.0	92.4	180.0	92.6
10	88.0	180.0	90.9	180.0	91.2
11	86.4	180.0	89.7	180.0	89.8
12	85	180.0	88.8	180.0	
13	-	-[d]	87.9	180.0	-
14	-	-	86.9	180.0	-
15	-	-	86.0	180.0	-
16	-	-	≅85	180.0	-

[a] Columns 2 and 3: small- and large-angle turning points for v_2 bending progression of HCN with $v_1 = 0$. Columns 4 and 5: small- and large-angle turning points for DCN, $v_1 = 0$; column 6, small-angle turning points for DCN, $v_1 = 1$. Number of decimal places in angles should not be taken too seriously. [b] For turning points indicated to be 180°, there *are* no turning points in the large-angle direction; angle θ decreases after H (D) atom "crosses the hump" at 180°. [c] Blank space in this column indicates no significant difference from corresponding value in column 3. [d] "-" indicates state corresponding to the particular set of quantum numbers is completely dissociated.

bending energy corresponds to (Table II) $97° \leq \theta \leq 180°$ for HCN. Does our surface "fit" this experimental observation? From Table I we see that $v_1 = 0$ HCN, which has 1140 cm^{-1} of stretching energy, should predissociate only when θ reaches $\simeq 100°$. From Table II, we see that $\theta \simeq 100°$ does indeed correspond to $v_2 = 4$. For lower values of v_2 (angles closer to 140°), the $v_1 = 0$ energy lies below the dissociation limit, so no predissociation occurs. Tables I and II also indicate that near 80–85° the $v_1 = 0$ energy (1140 cm^{-1}) should exceed the barrier height; at this point, predissociation should cease and pure dissociation (diffuse spectral features) should begin. θ values of 80–85° correspond to $v_2 = 12$–17; experimentally,[1] the structure in the photofragment spectrum disappears near $v_2 = 13$. Thus, although our surface predicts termination of predissociation at too large a v_2 value, qualitative agreement with experiment is good so far.

Let us now consider the $v_1 = 1$ progression in HCN where we have about 3410 cm^{-1} of stretching energy. According to Table I, if θ lies between 120° and 160° $v_1 = 1$ HCN should neither predissociate nor dissociate. From Table II we conclude that the $v_2 = 0$ and $v_2 = 1$ states of HCN should be *bound*. The $v_2 = 2$ state might be expected to be either purely dissociative or else very rapidly predissociated since its small-angle turning point ($\theta = 108°$) corresponds to a barrier of about 3400 cm^{-1} which is close to the $v_1 = 1$ energy (3410 cm^{-1}).[14] The $v_2 = 3$ state should be completely dissociated. Experimentally, none of the v_2 vibrational states are seen to give rise to *predissociation* structure. The photodissociation behavior of $v_1 = 0$, 1 C-state HCN, then, seems to be fairly well explained by our model.

Let us now analyze the spectral features of DCN. For $v_1 = 0$ we have $\simeq 750$ cm^{-1} of energy in the D--CN stretching coordinate. This means (Table I) that $v_1 = 0$ should remain bound until θ approaches 98–100° which corresponds (Table II) to $v_2 = 5$ or 6. However, near $\theta \simeq 100°$, the barrier height is 3230 cm^{-1}. The probability of DCN tunneling through a barrier of height 2480 (=3230 − 750) cm^{-1} and thickness 0.5 au is about 0.011 per D--CN vibration. This corresponds to a rate of about 2×10^{11} s^{-1}, which is somewhat slower than the rotational rate of DCN. Thus we expect the rate of tunneling to be slow at $v_2 = 5$. Experimentally, predissociation is seen to *begin* near $v_2 = 6$ with some evidence that lower members of the progression ($v_2 = 5$, 4) are also present. At $v_2 = 16$ the progression ends. From Table II we see that v_2 much larger than 16 corresponds to $\theta \simeq 85°$ where the barrier height is comparable to 750 cm^{-1}; again our surface is in agreement.

Next, we examine the v_2 progression for $v_1 = 1$ (which has 2200 cm^{-1} of D--CN stretching energy). Using Tables I and II, we see that predissociation should start near $v_2 = 4$ (at the 168° turning point); experimentally, it begins[1] at $v_2 = 5$. Our surface indicates that this v_2 predissociation progression should end at $v_2 = 12$ ($\theta \simeq 88°$) when the barrier height is comparable to the v_1 energy. Experimentally, it ends at $v_2 \simeq 11$.

At first glance, the model seems to break down for higher values of v_1 for DCN. For $v_1 = 2$ (which has 3600 cm^{-1} of stretching energy), Tables I and II predict predissociation to begin and end at $v_2 = 2$. Experimentally, the lower v_2 members of the $v_1 = 2$ DCN progression are obscured by other bands, but there seemed to be evidence in the Simons and MacPherson experiment[1] of at least the $v_2 = 7$, 8, 9 peaks. However, Table 2 of ref 1 shows exact degeneracy of the three DCN states ($v_1 = 2$; $v_2 = 7$, 8, 9; $v_3 = 0$) with the corresponding three states ($v_1 = 0$; $v_2 = 12$, 13, 14; $v_3 = 0$). Our model cannot rationalize predissociation for $v_1 = 2$, $v_2 = 4$, 5, ... let alone the $v_1 = 3$ progression which Simons and MacPherson also tentatively assigned (which would have about 5000 cm^{-1} of stretching energy). Rather, Table I predicts direct dissociation for $v_1 = 3$ DCN for *any* value of v_2.

The interpretation of the DCN $v_1 = 2$ data therefore presents a problem (it is probably excusable to regard the $v_1 = 3$ data as inconclusive since assignment was only tentative[1]). Our surface indicates that at $\theta \simeq 92°$ (the turning point corresponding to $v_2 = 9$ for DCN) the barrier height should be only 2600 cm^{-1}, far less than is needed to contain the 3600 cm^{-1} of stretching energy in $v_1 = 2$ DCN, whereas somewhat *less* energy in the stretching mode for HCN (3410 cm^{-1}) gives rise to very rapid dissociation even for $v_2 = 3$ (barrier height 3300 cm^{-1} at turning point of $\simeq 103°$).

There are several possible explanations which come to mind. First, the experimental data for DCN pertaining to the $v_1 = 2$ (and $v_1 = 3$) progression may have been misassigned. We recently communicated our findings to Professor Simons. He conceded[15] that there may have been just such a misassignment in this very difficult case. The assignment of the $v_1 = 2$ DCN peaks, which overlap members of the $v_1 = 0$ progression, was made as much on peak intensity as on band positions. It is possible that these intensities are perturbed by the strong B-, C-, and D-state interactions. Intensity contributions appearing to be due to $v_1 = 2$ might really be perturbed $v_1 = 0$ intensities.

Second, it could be that our computed barriers are too small for small angles ($\theta < 100°$) so that $v_1 = 2$ DCN actually lies below the barrier's peak. However, substantial changes in our surface would destroy the agreement our model gives for $v_1 = 0$, 1 HCN and $v_1 = 0$, 1 DCN.

A third possibility is that there exists an efficient energy redistribution mechanism in DCN which does not exist in HCN. One might imagine that the CN vibration in DCN ($v_3 \simeq 1600$ cm^{-1}) could couple strongly to the C--H stretch ($v_1 = 1465$ cm^{-1} for DCN), whereas such coupling would be weaker in HCN ($v_3 = 1745$ cm^{-1}, $v_1 = 2273$ cm^{-1}). In this case, it might be possible for vibrational excitation of the $v_1 = 2$ mode of DCN to redistribute part of its energy to the v_3 mode thereby reducing H--CN stretching energy and making the state stable on a predissociation time scale (order of a vibrational period). Also, the exact degeneracies noted earlier for the states (2; 7, 8, 9; 0) and (0; 12, 13, 14; 0) might couple the bending and stretching modes to such an extent that viewing the motion in terms of separate modes is misleading.

As an objection to the last two possibilities, we merely note that our potential surface and model gave such a nice interpretation of HCN and $v_1 = 0$, 1 DCN that we think further experimental study of $v_1 = 2$, 3 DCN is warranted.

Summary and Conclusions

We think that our ab initio calculated C-state potential-energy surface for HCN has given us an improved interpretation of the Simons and MacPherson photofragmentation data,[1] one *not* relying on two parallel dissociation pathways. Instead, we interpret the data in terms of a simple model in which excitation of the bending vibration allows the stretching motion to sample a variety of different tunneling barriers. Near $\theta = 140°$, the radial potential has no barrier so that R(H--CN) motion is either bound or purely dissociative (depending on whether the stretching energy is less than or greater than 4500 cm^{-1}). As the bending motion is excited, and the H atom moves away from $\theta = 140°$, the radial potential-energy curves have barriers which can give rise to predissociative behavior. As the bend is further excited, the barrier heights are found to decrease. For a given energy in the stretching mode, if one excites the bending mode to high enough energy, first tunneling and eventually purely dissociative motion become possible.

Appendix 1. Least-Squares Interpolation of Energy Surfaces

Our ab initio CI energies were fit to an interpolator by a least-squares approach. Because this is, to our knowledge, the

(14) A simple "square barrier" estimate of the tunneling rate indicates that a barrier thickness of 0.5 au (reasonably consistent with the potential curves of Figure 4) and a barrier height (top of barrier minus energy of vibration) of 100 to 1000 cm^{-1} should give tunneling probabilities of about 0.53–0.14 per H--CN vibration. The vibrational frequency of the H--CN stretching mode is about 6.8×10^{13} s^{-1} (4.35×10^{13} s^{-1} for DCN). Hence if the $v_1 = 1$, $v_2 = 2$ state were only 100 cm^{-1} or so below the barrier, the rate of predissociation ($=0.53 \times 1.5 \times 6.8 \times 10^{13}$ s^{-1} or $\simeq 5 \times 10^{13}$ s^{-1}) would be fast enough to make this line *very* diffuse and of very low polarization retention (recall that both HCN and DCN have rotational periods of about 2×10^{-13} sec).

(15) J. P. Simons, personal communication.

first use of a least-squares version of the interpolation technique of Downing et al.,[10] we think it is appropriate to discuss the method in some detail. The model secular equation[10] used to simulate the avoided crossing of two configurations is given as follows:

$$(H_{11} - E)(H_{22} - E) - (H_{12}H_{12}) = 0 \quad (1)$$

or

$$E^2 - E(H_{11} + H_{22}) + (H_{11}H_{22} - H_{12}^2) = 0 \quad (2)$$

The two solutions are

$$E_{\pm} = \{(H_{11} + H_{22}) \pm [(H_{11} + H_{22})^2 - 4(H_{11}H_{22} - H_{12}^2)]^{1/2}\}/2 \quad (3)$$

Downing et al.[10] have put forth a more general version of this procedure which yields an Nth-order polynomial in E. Since we wish to model the avoided crossing of pairs of states only, the quadratic problem is probably the most meaningful here.

In the quadratic energy eq 2, the CI matrix elements H_{ij} are functions of the two H-atom coordinates (recall that we fix the bond length and location of the CN fragment for all calculations). Following Downing et al.,[10] we express the specific combinations of H_{ij} matrix elements appearing in eq 2 as polynomials P, Q in the two H atom geometrical coordinates:

$$-(H_{11} + H_{22}) = P(x,y) \quad (4)$$

$$(H_{11}H_{22} - H_{12}^2) = Q(x,y) \quad (5)$$

Here x and y are relevant coordinates of the system (R(H--CN) and θ, or the x and y coordinates of the H atom, for example), and P and Q are Laurent series in these coordinates. The unknowns, of course, are the expansion coefficients of P and Q pertaining to various powers of x and y. Since one does not generally know the "natural" or optimal coordinates in terms of which to expand the H_{ij} matrix elements, it is often necessary for P and Q to contain many powers of the coordinates (including cross terms) and, hence, many unknown parameters. To keep the number of fitting parameters small (and presumably to thereby increase their numerical significance), a least sum of squares (LSS) approach was used to choose the best parameters in P and Q to fit our ab initio energies to eq 2.

Combining the last two terms in eq 2 by noting their polynomial nature, and writing the exponents and coefficients explicitly, we have

$$E^2 + \sum_{\alpha} a_{\alpha}E^{i_\alpha}x^{j_\alpha}y^{k_\alpha} = 0 \quad (6)$$

Given the energy E at any geometry (x,y) the unknowns in eq 6 are the coefficients $\{a_\alpha\}$. We represent this equation symbolically as follows:

$$E^2 + \zeta(E,x,y) = 0 \quad (7)$$

Now we define, in analogy with the usual least-squares procedure,

$$\mathrm{LSS} = \sum_{\mathrm{A}} \{E_{\mathrm{A}} + \zeta(E_{\mathrm{A}},x_{\mathrm{A}},y_{\mathrm{A}})\}^2 \quad (8)$$

where E_{A}, x_{A}, and y_{A} are the *known* input (energy and coordinate) data points. Defining $\zeta(\mathrm{A}) = \zeta(E_{\mathrm{A}},x_{\mathrm{A}},y_{\mathrm{A}})$, we next minimize LSS with respect to a particular parameter a_β:

$$0 = \frac{\partial \mathrm{LSS}}{\partial a_\beta} = 2\sum_{\mathrm{A}}\{E_{\mathrm{A}}^2 + \zeta(\mathrm{A})\}\frac{\partial \zeta(\mathrm{A})}{\partial a_\beta} \quad (9)$$

which leads to a set of linear equations for the unknown expansion coefficients $\{a_\alpha\}$:

$$\sum_{\alpha}\{\sum_{\mathrm{A}} E_{\mathrm{A}}{}^{i_\alpha+i_\beta}x_{\mathrm{A}}{}^{j_\alpha+j_\beta}y_{\mathrm{A}}{}^{k_\alpha+k_\beta}\}a_\alpha = -\{\sum_{\mathrm{A}} E_{\mathrm{A}}{}^{i_\beta+2}x_{\mathrm{A}}{}^{j_\beta}y_{\mathrm{A}}{}^{k_\beta}\} \quad (10)$$

The main advantage of the quadratic fitting method[10] is that one can utilize information from two states of the molecular system and obtain, for a given geometry, one equation in E whose *two* roots are the energies of the states. That is, that the quadratic energy equation has "avoided crossing" behavior built into it. Since we use a LSS fitting approach, we can also look for the "most natural" coordinates for the problem by searching for the interpolator with the fewest parameters that reproduces the input energy values to some acceptable tolerance.

After some experimenting, we found that an interpolator involving polynomials in R(H--CN) and cos θ gave a reasonable least-squares fit to our ab initio data (the average magnitude of the deviation from the input points being 16 cm^{-1}). This interpolator was then used to generate the C-state energy at intermediate geometries.

Appendix 2. Configuration Selection Procedure

The philosophy of our "configuration selection" method is to include in the configuration list enough single and double excitations to "relax" the orbitals (to allow for their variable quality at different geometries) and to correlate the electrons about equally well at all of the nuclear configurations of interest. We chose several "test" geometries, including two near the equilibria of the B and C states (as given by Schaefer et al.[8]), some "bond-breaking" distances where the H--C bond is only partly formed, and a few highly distorted geometries at which we expected configuration crossings to occur.

We first performed CI calculations including single and selected double excitations from the occupancy of the X $^1A'$ ground state (freezing the "core" nitrogen and carbon 1s orbitals and the C--N σ bond). The magnitudes of the expansion coefficients in the B- and C-state eigenvectors were then classified as "large" (>0.10), "medium" (0.05–0.10), or "small" (<0.05). A configuration list was then constructed which included all of the "large" coefficient configurations for *both* the B and C states (at all seven geometries) plus all single and low-lying double excitations from these configurations. Next, the "medium" coefficient configurations (again, with respect to both the B and C states, and at all seven test geometries) were included in the list and *all* single excitations from them were added to the list. Of course, some of these latter configurations had already been included as single or double excitations from the "large" configurations. A unitary group based distinct row table (DRT) was then constructed which included all configurations detailed above.

The classification of "large", "medium", or "small" as based on the tolerances 0.10 and 0.05 was the best we could do using the existing computer routines and facilities at Utah. We felt that a configuration list which included all important single and double excitations relative to the "large" reference configurations plus single excitations relative to the "medium" reference configurations represented a physically reasonable trial CI wave function. Attempting to include more than the few thousand most important configurations, in light of the modest size of our Gaussian orbital basis set, was not considered a worthwhile effort.

With use of the trial DRT outlined above, a new unitary group CI calculation was performed, and the eigenvectors of this (larger) CI were examined. From these CI expansion coefficients, a new configuration list was again constructed that included all "large" coefficient configurations and all single and low-lying double excitations from them, and all "medium" coefficient configurations and all single excitations from them. Another CI calculation was then performed, and this procedure was continued until the configuration list "converged".

The resultant DRT gave rise to a CI matrix which was not economically feasible to use for calculating a global surface (150 or so geometries), so we systematically reduced the dimension of the CI space by discarding those excitations which put electrons into the higher energy virtual orbitals. While doing so, we compared the resultant (smaller CI) energies at our test geometries to those obtained from the larger "converged" configuration list. After some comparison, we found a 2488 configuration CI wave function which gave the same shape to the B- and C-state energy surfaces at the seven test geometries (±2.5 kcal/mol) as the larger CI wave function. This final wave function was then used to generate the configuration list for *all* of the subsequent CI calculations whose results are presented in this paper. Perhaps the

strongest argument for the quality of the CI energies given by this wave function is the good agreement of the experimental[1] data and our predictions based on this CI surface.

Acknowledgment. We acknowledge support from the National Science Foundation (Contract No. 7906645, as well as partial support of the Utah DEC 2060 computer on which all of these calculations were carried out). We also thank Professor J. Michl for stimulating discussions concerning the need for interpretation of the HCN data.

Registry No. HCN, 74-90-8; DCN, 3017-23-0.

Infrared Photochemistry of $[(C_2H_5)_2O]_2H^+$ and $C_3F_6^+$. A Comparison of Pulsed and Continuous-Wave Laser Photodissociation Methods

Joseph M. Jasinski, Robert N. Rosenfeld, Felix K. Meyer, and John I. Brauman*

Contribution from the Department of Chemistry, Stanford University, Stanford, California 94305. *Received December 15, 1980*

Abstract: A versatile technique employing pulsed ion cyclotron resonance spectroscopy and a pulsed CO_2 laser to study the megawatt infrared multiphoton dissociation of gas-phase ions under collisionless conditions is described. Wavelength and fluence dependences are reported for the ions $[(C_2H_5)_2O]_2H^+$ and $C_3F_6^+$. These results are compared with previous low-power infrared photodissociation studies of these ions carried out by using a continuous-wave CO_2 laser. The results for both continuous-wave and pulsed laser excitation are qualitatively similar; however, differences are found in the magnitude of the photodissociation cross sections for both ions and in λ_{max} of the photodissociation spectrum of $C_3F_6^+$. Possible reasons for these differences are discussed.

We have recently developed a method for studying the infrared (IR) multiphoton photochemistry of gas-phase ions.[1-4] A pulsed ion cyclotron resonance (ICR) spectrometer is used to generate, trap, and mass spectrometrically detect either positive or negative ions. Infrared photochemistry is induced by irradiating the trapped ions with the output from a pulsed TEA CO_2 laser. We have employed this technique in studying the photophysics of the multiphoton dissociation process,[1,2] in probing vibrational relaxation in gas-phase ions[2,3] and in demonstrating that some anions undergo an electronic transition, electron photodetachment, upon IR multiphoton absorption.[4] This paper provides a detailed description of the experimental techniques and data analysis employed in our photodissociation studies and presents data on the wavelength and fluence dependences of the ions $[(C_2H_5)_2O]_2H^+$ and $C_3F_6^+$.

Most of the information currently available on IR multiphoton processes comes from numerous studies on neutral systems employing a variety of experimental techniques for irradiation, product detection, and yield determination.[5] Such studies have elucidated a number of important aspects of the multiphoton absorption and dissociation process. They have also demonstrated the need for carefully controlled experimental conditions if the data obtained are to be useful in understanding the photophysics of IR multiphoton processes. In particular it is desirable to conduct experiments at low pressures, where collisional effects are unimportant, and under conditions where secondary reactions of photoproducts and wall-catalyzed reactions are minimized. Our technique provides these as well as several other desirable experimental features. Typical ICR operating pressures are in the 10^{-8}-10^{-5} torr range. At these pressures the time between ion-neutral collisions ranges from 3 s to 3 ms, much longer than the 3 μs laser pulse and in general longer than the relevant time scale for IR multiphoton dissociation induced by such a pulse.[6] Thus, to a very good approximation, we can study IR multiphoton dissociation in the absence of complicating effects due to collisions. Detection of products and determination of the photolysis yield is carried out after a single laser pulse, thus minimizing secondary reactions, and in most cases all ionic products can be readily identified. Furthermore, because the experiment is time resolved on a millisecond time scale, unimolecular decomposition products are easily distinguished from species formed bimolecularly. Wall-catalyzed processes are rigorously excluded since an ion-wall collision results in the ion being neutralized and removed from the experiment. Finally, because the duty cycle of the entire experiment is 1 s, species with rather low decomposition thresholds which would be impossible to work with under most conditions can be readily generated and photolyzed. This allows us to study IR multiphoton dissociation in the limit of extensive decomposition per pulse—a regime which is important in obtaining a complete understanding of multiphoton dissociation but which is often not accessible in experiments on more stable neutral species. In addition, we are able to employ a collimated laser beam of only modest peak intensity (10-15 MW cm^{-2}), thereby obviating many of the experimental difficulties inherent in the use of tightly focused laser beams.

In contrast to the large amount of work which has been done on IR multiphoton dissociation of neutrals, relatively few studies have thus far been carried out on gas-phase ions. Von Hellfeld et al. have reported data on the dissociation of SF_5^+ using a crossed ion beam-TEA CO_2 laser beam apparatus;[7] however, most pre-

(1) Rosenfeld, R. N.; Jasinski, J. M.; Brauman, J. I. *Chem. Phys. Lett.* **1980**, *71*, 400.

(2) (a) Rosenfeld, R. N.; Jasinski, J. M.; Brauman, J. I. *J. Am. Chem. Soc.* **1979**, *101*, 3999. (b) Rosenfeld, R. N.; Jasinski, J. M.; Brauman, J. I., *Ibid.*, following paper in this issue.

(3) Jasinski, J. M.; Brauman, J. I. *J. Chem. Phys.* **1980**, *73*, 6191.

(4) Rosenfeld, R. N.; Jasinski, J. M.; Brauman, J. I. *J. Chem. Phys.* **1979**, *71*, 1030.

(5) For recent reviews, see: (a) Schulz, P. A.; Sudbo, Aa. S.; Krajnovich, D. J.; Kwok, H. S.; Shen, Y. R.; Lee, Y. T. *Annu. Rev. Phys. Chem.* **1979**, *30*, 379. (b) Cantrell, C. D.; Freund, S. M.; Lyman, J. L. In "Laser Handbook"; Stitch, M. L., Ed.; North-Holland Publishing Co.: Amsterdam, 1979; Vol. III, p 485.

(6) This conclusion follows from the fact that in general the unimolecular dissociation rate will be greater than or equal to the rate of photon absorption at or above the dissociation threshold. The rate of photon absorption at typical pulsed CO_2 laser intensities (unfocused, in the megawatt range) is expected to be 10^6-10^9 s^{-1}. Thus for a typical 3-μs laser pulse most of the decomposition will occur during or shortly after the laser pulse.

(7) Von Hellfeld, A.; Feldmann, D.; Welge, K. H.; Fournier, A. P. *Opt. Commun.* **1979**, *30*, 193.

0002-7863/82/1504-0652$01.25/0